γ-γ correlations in sodium-22 and cobalt-60 nuclear decays

Anthony Bader
Department of Physics and Astronomy, Stony Brook University
Stony Brook, New York 11794-3800, USA

The goal of the experiment was to determine the angular correlation of emitted photons from the cobalt-60 (^{60}Co) beta decay nuclear transitions. As the angular correlation of emitted photons during successive angular momentum states of the decayed ^{60}Co nuclei were complex relations based on the Legendre polynomials, a test run of a simplified angular correlation — namely, that of sodium-22 (^{22}Na) — was conducted as a preliminary experiment. Varying the angle between the two detectors allowed for a measurement of counts as a function of angle for relative time frames. For ^{22}Na the value of R^2 was 0.9056, indicating a reasonable fit. For ^{60}Co the value of R^2 was 0.4492 with only the a_2 and a_4 coefficients as a part of the estimation and an R^2 value of .6973 with the P_1 term added. The angular coefficients were $a_2 = 0.0588 \pm .0113$ and $a_4 = 0.0072 \pm .0117$. The small R^2 values shows the lack of strong fit, and these values for the angular coefficients do not match one of the expected decay sequences. [1]

I. INTRODUCTION

A. Historical Relevance and General Theory

The laboratory study and techniques employed in angular correlation measurements have been of great importance to the history of physics, particularly with experimentation. From the standpoint of theory however, the angular correlations shown in nuclear decays, such as the ones studied, have allowed for confirmation of the quantized nature of angular momentum at the subatomic scale. The property of angular momentum is fundamentally quantized at the atomic and subatomic level, in analogy to various other properties studied in quantum mechanics. Unlike other fundamental quantities such as linear momentum and position, the property of angular momentum is comprised of multiple quantities obeying the uncertainty principle (i.e. position and momentum), thus it always bears an indeterminate value.

Coincidence counting is utilized in this lab, which has been a technique pivotal to experiments in quantum mechanics. An example of a system of momentum that an experimenter may wish to analyze is particle and anti-particle collision, where annihilation should be considered instantaneous. The result will be photons striking the detectors in tandem; however, there may be radiation from the system striking the detectors causing false positives in any measurement. Many other physical systems bear this relationship, such as entangled particles. A coincidence counter corrects for this by correlating emission times with detection times, removing unwanted detections from a series of measurements. This is not only important for obtaining measurements of desired particles in general, but essential to experimental accuracy, as the ratio of particles of interest to total particles in a system is often very small. As there is a limit to time precision in any physical experiment, only time intervals where something can be considered coincident can be used. This is referred to as the resolving time. To improve the ratio of true to false coincidences, the resolving time would be further decreased, as has been done throughout various experiments utilizing coincidence counting.

B. Sodium-22 Beta Decay

In the lab ^{22}Na angular correlations were used as a preliminary step to analyzing the ^{60}Co angular correlations. As ^{22}Na is a positron emitting source, the sodium sample will convert protons in the sample nuclei into neutrons. A by-product of this for any given atomic nucleus in the sample is the emission of a positron and neutrino. This is β^+ decay, which in general is given as,

$$(Z, N; A) \rightarrow (Z - 1, N + 1; A) + e^+ + \nu_e \qquad (1)$$

where Z is the number of protons, N is the number of neutrons, and $A = Z + N$, for some element X, notated as ${}^A_Z X$. In the case of ^{22}Na, this becomes

$$^{22}_{11}\mathrm{Na} \rightarrow ^{22}_{10}\mathrm{Ne} + e^+ + \nu_e.$$

While there is a much more complex angular interaction with respect to the cobalt sample, the positron emission of the sodium sample can be used as a proxy for a simplified angular correlation. Once emitted, the positrons in the ^{22}Na sample will collide with nearby electrons; this causes annihilation of the particle anti-particle pairs resulting in the creation of two high energy photons. As the photons are by-products of matter-antimatter collision, the respective linear momenta of the previous particles need to be conserved; thus the photons will propagate at 180 degrees from each other. This only holds true on the assumption that the linear momenta of the particles are similar in magnitude, which is likely to be the case as a small ratio in magnitude of linear momenta is usually necessary for annihilation to occur in the first place. In theory if the detectors were point masses in space with zero area, a δ distribution about 180 degrees would be the true spread of counts as a function of angle

(in the lab the θ value was measured as a displacement from the 180 degree line making these values 0 degrees). [1]

C. Cobalt-60 Decay

When nuclear transitions occur in a given radioactive sample, such as ^{60}Co in the experiment, there will be an angular correlation between the observed photons emitted. A sample of ^{60}Co decays to Nickel-60 (^{60}Ni) via the process of β^- decay unlike the decay mentioned in 1, this is described by,

$$^{60}_{27}\text{Co} \rightarrow ^{60}_{28}\text{Ni} + e^- + \bar{\nu}_e$$

Representing the angular momentum of any given decayed sample nucleus as J, the new ^{60}Ni nuclei will remain in a state J (units of $\hbar$), which is unstable for a time before transitioning to J' an even more unstable state which will serve as the intermediate state between J and the ground state.[1]

One example of this J to J' to ground state transition is the transition J = 4 to J = 2 and from J = 2 to J = 0 (the ground state which exhibits no preferred orientation in space). This is a particularly relevant example to work with as it is the experimentally expected transition pattern. Upon each transition, a specific energy photon will be emitted. The J = 2 angular momentum state is then defined as the intermediate transition state, being the most unstable of those analyzed in the experiment. It is important to note that this state lasts for approximately one picosecond while the J = 4 state lasts about six orders of magnitude longer; this allows the experimenters to define the two consecutive photon emissions as simultaneous with such a short relative time lapse occurring in the J = 2 transition. The angular correlation comes about by conservation of angular momentum, as each photon carries with it an angular momentum distribution, with a total angular momentum of 2 defined as S. If one defines the emission of the first photon as the z-axis the component S_z can take one the values ± 2 while the total angular momentum of the atomic nucleus has a component J_z with the possible values -2,-1,0,1 and 2 after the first photon's emission. The process continues with the second photon emission occurring at some arbitrary angle from the new defined angular momentum of the nucleus, which also bears a total angular momentum of 2 with S_z having the possible value -2,-1,0,1 and 2. The angular correlation of the gamma ray defined as $Y(\theta)$ now comes about by the total angular momentum of the system originally with J = 4 and no spin bearing photons, to J = 0 with two emitted photons conserving the total angular momentum. $Y(\theta)$ here is a measure of the number of counts, recorded simultaneous emissions, as a function of θ, the angle at which the detecting devices are separated by. If the first photon was emitted at some angle θ with respect to the axis of the nucleus, this weighs in the distribution of position of the new axis of the nucleus at some angle angle ϕ from the first axis along the first emitted photon. The second photon bears its own angular distribution about the new axis defined at ϕ, thus its angular displacement from the original θ now has a defined probability; this θ value can be considered the angular coincidence between the two photons. Since the Legendre polynomials are eigenfunctions of angular momentum and the spin and angular momentum of the system are what gives rise to the angular correlations between the emitted gamma rays, the correlation term $Y(\theta)$ is expressed in terms of Legendre polynomials. [1] Expanded this gives the expression,

$$Y(\theta) = \sum_{l=0}^{4} A_l P_l(cos(\theta)) = A_0 + A_1 P_1(\cos(\theta)) + A_2 P_2(\cos(\theta)) + A_3 P_3(\cos(\theta)) + A_4 P_4(\cos(\theta)) \quad (2)$$

The nuclear transitions have their own respective parities which are conserved, making the correlations symmetric about 90°; therefore only even terms in the Legendre polynomials are relevant. The values of significance in the lab are then the Legendre coefficients A_0, A_2, and A_4. After factoring out the A_0 the new terms of relevance are defined as a_2 and a_4.

II. EXPERIMENTAL SETUP

A. Photomultiplier

A crucial piece of the laboratory setup was the use of a photomultiplier, which was integrated into the electronics. Two 1 and 3/4 in x 2 in NaI(Tl) scintillation counters are bonded to the photomultipliers; this is a quite common practice as it increases the overall efficiency of the photomultipliers. A high energy incident photon comes into contact with the scintillator, in lab the high energy photon is the emitted gamma ray from either the ^{60}Co or ^{22}Na sample. Once passing through the scintillator the ionization track emits several photons now bearing less energy than the original single high energy incident photon. These photons then come into contact with a photocathode, a material that has been coated as to insure a high photo-sensitivity. From the photoelectric effect, these incident lower energy photons (now usually in the visible wavelength range) overcome the work function of the photocathode thus, ionizing an electron. Now the newly freed electron will be pulled by the electric field generated by the potential difference established within the vacuum enclosure, with a greater potential difference between each respective dynode. The dynodes are designed so that high translational energy contact with an incident particle, here an electron, allows for secondary emission. Secondary emission is the process by which a greater number of electrons are "freed" from the dynode source after collision, creating a stream of free electrons. As the chamber is nearly a vacuum, unwanted

collisions between the electrons and gaseous particles is highly unlikely. This occurs over several iterations, allowing for a cascading effect with electrons moving towards the anode, where a new dramatically increased current can be detected. This is where the photomultiplier becomes particularly useful, as one can now work with readable current and voltage values detectable by most lab equipment, while simultaneously being able to analyze emissions of single high energy photons.

B. Laboratory Electronics

Experimentally removing noise from data collection was needed to analyze the nuclear decay processes in the lab. To measure the angular correlations with gamma ray emissions, two Timing Signal Chanel Analyzers, abbreviated TSCAs were used for the radiation detectors. The TSCAs are able to gauge incident energy pulses from the photomultiplier, sorting them into bins parsed by their energy levels. With 2048 bins, the plot of these bins is effectively a frequency of occurrence as a function of energy level. This plot can be utilized to narrow the energy range of the incident pulses, removing any signals outside a visible distribution seen in the plot of frequency vs energy level. It is important to note that this is a preliminary step, this graph does not allow one to note anything about the photon energies, given that any detected energy has been heavily amplified by the photomultiplier.

The second key piece of the electronics in the setup is the Time Amplitude Converter (TAC). The logic pulses sent from TSCAs go to the TAC, with an artificially created time delay from the mobile detector's TSCA. The TAC acts as a measuring device for the time separation of the two TSCAs. The TAC initiates once the TSCA from the stationary detector is struck by one of the logic pulses and stops when the TSCA from the mobile detector is struck. With simultaneity as a requirement for coincidences, the time delay between an successive logic pulses should be constant. This is true for both the ^{22}Na decay which is actually simultaneous and the ^{60}Co decay which is very well approximated as an instantaneous process. Because of this, the frequency of delay times will spike for the true coincidence measurements, allowing one to estimate any unintended recordings.

A 13-Bit ADC, which serves as a multi-channel analyzer with the addition of the binning routine, sends the TAC and TSCA outputs to the MAESTRO program. The MAESTRO program allows the experimenter to analyze data input from the TAC and TSCAs to the connected computer. It renders the signal amplitudes to one of the 2048 available energy bins, with heavily amplified photon energies for the TSCAs and delay times from the TAC. MAESTRO serves as a histogram generator of the data, allowing the experimenter to see the data in real time and note the signals and noise received.

C. Angular Corrections

From the theory detailed above, the ^{22}Na angular correlations should follow a δ distribution with the detectors 180 degrees apart (i.e. $\theta = 0$). However, this assumes the radiation source is a point with two point detectors. The expected values for the ^{22}Na sample could then be accounted for by taking into account the surface areas for the detectors and any other geometric constituents in the lab.

As the radius of the detectors R and the distance from them to the sample L are both significantly larger than the small radius of the sample, the ^{22}Na source is well approximated as a single point in space. As the mobile detector changes its angular position, less of the surface area is exposed to incident photons as they can only travel 180 degrees apart from their source of creation. Mathematically the flux of incident photons can then be analyzed for the various θ values by looking at the one to one mapping of points along the surface areas of the detectors, expressed in terms of the mobile detectors position. Thinking of the mobile detector as a disk, the exposed area will be charted out by a chord that intersects the x axis, at some point r which can vary from 0 to $2R$. The exposed portion of the surface area of the detector can then be expressed as,

$$A = \int_0^r \sqrt{2xR - x^2}dx \tag{3}$$

The value of r is a linear function of θ when the detector is anywhere from $\theta = 0$ to $\theta = \frac{2R}{L}$ described by,

$$r = 2R - L\theta \tag{4}$$

Thus, one can see for the value of $\theta = 0$, the value of r can sweep across the x positions up to $2R$, with $r = 2R$. When the detector is at a $\theta = \frac{2R}{L}, r = 0$, this would be the angle at which there is no longer any one to one mapping of points on the surface areas of the detectors. The final equation for ^{22}Na is the expected value for the number of counts, $C(\theta)$ as a function of θ, mapping the available surface area of the mobile detector. Thinking of the exposed surface area of the detector as a fraction of its available total area, πR^2, the following relation normalized by C_0,

$$C(\theta) = \frac{C_0}{\pi R^2} \int_0^{2R-L\theta} \sqrt{2xR - x^2}dx \tag{5}$$

The angular correction for ^{60}Co can be stated in terms of the Legendre Polynomials, which are corrected for by the Legendre coefficients a_i. The the actual angular correlation is given as,

$$Y_{true}(\theta) = \sum_l b_l P_l(cos(\theta)) \tag{6}$$

When accounting for the radius of the detectors and their distance from the ^{60}Co source, the experimental angular correlation is

$$Y(\theta) = \sum_l \left[\frac{J_l}{J_0}\right]_{det1} \left[\frac{J_l}{J_0}\right]_{det2} a_l P_l(cos(\theta)) \qquad (7)$$

with a_l as the theoretical values of the Legendre Polynomial coefficients for the decay transition. The factors, $[J_2/J_0]$ and $[J_4/J_0]$, which adjust the angular correlations, can be determined from the graphs for $[J_l/J_0]$ as piecewise functions of the distance from the detector to the source and the energy emissions included in the lab manual.

III. DATA ANALYSIS

A. Background Radiation Adjustments

As background radiation played a significant role in the data collection, the recording of false positive measurements (i.e. false coincidence measurements) had to be accounted for when analyzing the data. MAESTRO's time-amplitude-conversion output parses recordings into delay time bins, with a total of 2048 bins for collecting coincidence measurements. The detectors ran for approximately 10 minutes for each angle when collecting data for ^{22}Na. Because this could be completed within one lab session, the time discrepancies were minuscule, with all values normalized to 10 minutes. The recording times varied quite extensively when taking data for ^{60}Co, as the detectors were left to run over the duration of one to two nights. The coincidence recordings were then adjusted to the average hourly number of recorded counts for each angle.

To estimate the number of false coincidences in the data set for each angle, the bins with low count values in each set were designated as sources of error. This is because the bins with high count values formed clear distributions about a mean value having the greatest number recorded coincidences. Bins with low count values, particularly those that fell outside of the distribution, were almost entirely false coincidences. One could then obtain an estimate of the number of true coincidences, c(n) by summing over bins with a count threshold n. The best way to optimize n was to simply analyze the graph and bin data, eying which values of n would be enough to cover all counts outside of the distribution while keeping n small enough as to not remove true coincidences from the distribution itself. For ^{22}Na, $n = 3$ was ideal, while for ^{60}Co, which ran for substantially longer, a value of $n = 8$ sufficed. This value could be computed quickly by utilizing the "SUMIF()" function in excel, providing a useful estimate for true coincidences; however, it fails to account for false coincidence recordings in the actual distribution itself, particularly near the mean.

A more accurate account for false coincidences can be found by considering the the ratio of false coincidences

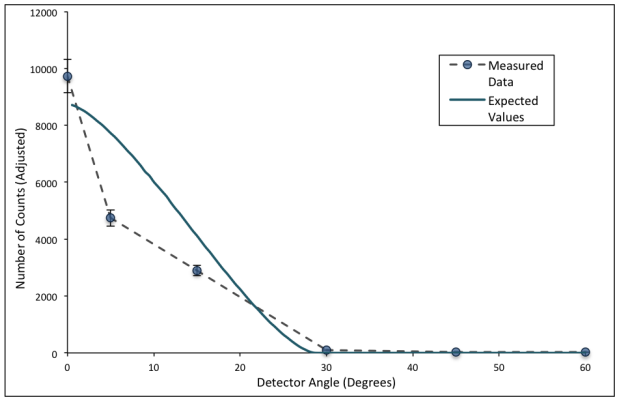

FIG. 1: ^{22}Na: modified total counts for each angle, with the theoretical distribution of coincidences

per bin summed over all bins. With N(n) as the number of bins with n or less counts, k(n) as the number of counts in all bins with n or less counts, then the average number of false coincidences per bin is $k(n)/N(n)$. This allows one to find the modified value for total coincidences c_m, a superior approximation to the number of true coincidences with a total number of counts $c(n = 0) = c_T$ as

$$c_m = c_T - 2048\frac{k(n)}{N(n)}. \qquad (8)$$

A good check is to see that $c_m \leq c(n)$ with $c_m \approx c(n)$.

B. Sodium-22 Angular Correlation

The ^{22}Na values for counts as a function of θ were plotted in Figure 1 showing the experimental values for the angular correlation as well as the expected values from the setup's underlying geometry. As to be expected the graph shows a clear monotonic descent consistent with theory, as less surface area of the detectors are exposed to radiation with increasing θ values. The errors in c_m, the modified values for true coincidences at each value of θ were found from its relationship with c_T. Since c_T describes counts as a random variable, with a consistent average "count rate" per unit time; c_T can modeled as a Poisson distribution. c_T then has a relative uncertainty of

$$\frac{\Delta c_T}{c_T} = \frac{1}{\sqrt{c_T}} \qquad (9)$$

As c_m is just a proportional measure of c_T, they share relative uncertainties, making the absolute uncertainty of c_m as see in figure 1

$$\Delta c_m = \frac{c_m}{\sqrt{c_T}} \qquad (10)$$

The distribution of the expected values of ^{22}Na for each angle was computed via a Riemann sum approximation

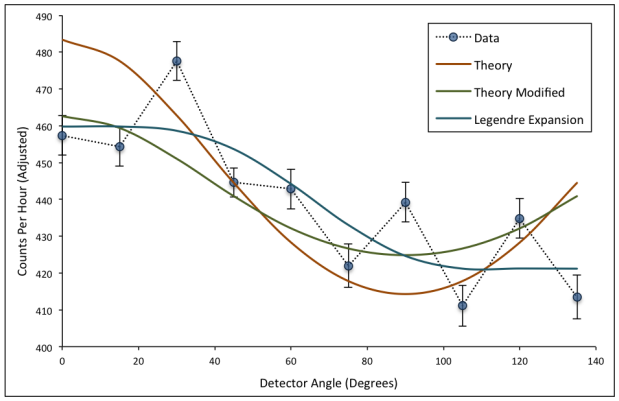

FIG. 2: ^{60}Co: Recorded counts at each angle, with theoretical distributions and modified fits from least squares regression analyses.

TABLE I: ^{60}Co obtained coefficients for different fits with coefficients of determination

Graph Fit	a_1	a_2	a_4	R^2
Theory	0	0.102000	0.009100	0.4489
Theory Optimized	0	0.055292	0.006085	0.4491
Theory Modified	0	0.058821	0.007245	0.4492
Legendre Expansion	0.05309	0.024600	-0.014200	0.6973

to equation 5. C_0 was optimized using "solver" in Excel with a least squares regression and C_0 as a free parameter. The initial value to pivot around was entered as $C(\theta = 0)$ with $C(\theta = 0) \approx C_0$. The coefficient of determination, R^2 was found to be .9056 for the the ^{22}Na fit, indicating a strong convergence with the data and theory. As seen in figure 1 the curve demonstrating the expected values as well as the collected data both drop off around 30 degrees, which is to be expected as this is approximately where the surface areas of the detectors are no longer exposed to anti-parallel photon emission from the ^{22}Na source.

C. Cobalt-60 Angular Correlation

Figure 2 shows the values obtained for the ^{60}Co angular correlation. The uncertainty in the modified counts were found with the same reasoning as the Δc_m value for ^{22}Na. The value $\Delta c_T/c_T$, the relative uncertainty of the total counts is approximately the same as the relative uncertainty $\Delta c_m/c_m$. Thus, one can obtain the value for Δc_m with,

$$\Delta c_m = \frac{c_m}{\sqrt{c_T}} \tag{11}$$

Figure 2 shows the collected data for the ^{60}Co J = 4 to J = 2, J = 2 to J = 0 decay cycle. As there are numerous parameters that can be adjusted for this portion of the lab, the best option is to try out multiple fits for the data. From theory, the transition has the coefficients $a_2 = 0.102$ and $a_4 = 0.0091$, when disregarding the geometry of the experimental setup (i.e no correction factors). This distribution is shown as "theory" in figure 2, which was computed by simply summing over the Legendre polynomials for each angle using the values $a_2 = 0.102$ and $a_4 = 0.0091$. The value for A_0, the normalization factor can be optimized with the solver function in Excel, treating A_0 as a free parameter for a χ^2 set of data. With,

$$\chi^2 = \sum_i \frac{(\text{Data}(\theta) - \text{Y}(\theta))^2}{(\text{Error}(\theta_i))^2} \tag{12}$$

the solver function optimizes the values of all free parameters to minimize the value of χ^2. This yields a poor coefficient of determination of only .4489 as seen in table 1. This can be enhanced by letting a_2 and a_4 be treated as free parameters in the χ^2 set of data. Using the solver function in Excel again, one could minimize the χ^2 value obtaining what is graphed as "Optimized Theory" with very slight improvement in R^2 having a value of .4491. The fit labeled "Theory Modified" is the same as "Theory Optimized," but with the angular correction factors input into the available data set. As this fit is nearly identical with "Optimized Theory," but slightly more accurate, it was included in figure 2, without inclusion of "Optimized Theory." This still holds a poor R^2 value of only .4492. The final fit labeled "Legendre Expansion" accounts for the angular correction factors and adds in the P_l term in the Legendre Polynomial summation. This adds an additional free parameter, a_1 for solver to work with, maximizing the fit even further. This provides an R^2 value of .6973, which is vastly superior to the others; however, still a fairly weak correlation overall.

While the coefficients of determination improved with each respective fit, this can easily be criticized as data over-fitting given the small sample of points. Noting the value of a_1 is also important in table 1, as it shows a fairly large value of .05309. This suggests the laboratory setup had some asymmetric aspects that were unaccounted for, as the a_1 term should be zero for the nuclear transition. Table 1 also shows the values for the coefficients a_2 and a_4 are much further away from the theoretical and expected experimental values in the fit including the a_1 term. Because of this, there are likely unaccounted for errors in the lab in addition to asymmetry in the experimental setup.

Evaluating the uncertainty in the coefficient measurements was done by utilizing solver using the 1σ uncertainty, (one standard deviation) method. The parameter was varied to minimize χ^2 with the constraint of $\chi^2(\text{min}) \rightarrow \chi^2(\text{min}) + 1$. This produced the uncertainty values for each coefficient with $a_1 = .05309 \pm .0086$, $a_2 = .0246 \pm .0107$, and $a_4 = -.0142 \pm .0112$.

IV. CONCLUSION

The results of the lab were ultimately unsuccessful in demonstrating the J = 4 to J = 2 and J = 2 to J = 0 transitions with the respective coefficients in ^{60}Co. While the preliminary step of analyzing ^{22}Na was far more successful than the experiment with ^{60}Co, there was not a full convergence with the collected data and expected values. The R^2 value of .9056 showed potential in the laboratory equipment and experimental design to detect angular correlations, as this coefficient of determination was far better than the ones obtained for ^{60}Co. The results were most likely skewed by some underlying asymmetry in the experiment that went unaccounted for, as the a_1 term was quite large. Having the detector operate at a greater number of angles would have been helpful in eliminating statistical outliers and error. This could have been done with MAESTRO recording over time intervals, with an automated mobile detector removing the need for a human operator at most angles.

[1] Melissinos, A. *Experiments in Modern Physics.* (New York, NY: Academic Press INC., 1968).